Supporting Information

Magnetic Field Driven Electron Dynamics in Graphene

Fatima[1,2], Talgat Inerbaev[3,4], Wenjie Xia[1*], Dmitri S. Kilin[2*]

[1]Department of Civil and Environmental Engineering, North Dakota State University, Fargo, North Dakota 58108, USA

[2]Department of Chemistry and Biochemistry, North Dakota State University, Fargo, North Dakota 58108, USA

[3]Sobolev Institute of Geology and Mineralogy, Siberian Branch, Russian Academy of Sciences, Novosibirsk 630090, Russia;

[4]L. N. Gumilyov Eurasian National University, Astana 010000, Kazakhstan

1. ORGANIZATION OF SUPPORTING INFORMATION

The Supporting Information Document is organized as follows. Section 2 introduces notations and overviews computational procedure. Theoretical background related to the tight-binding model is refreshed in subsection 2.1. Computational procedures related to the analysis of eigenstates in the magnetic field are summarized in subsection 2.2. Modeling approaches for quantum dynamics are explained in subsection 2.3. Observables and the format for analysis of the results are provided in subsection 2.4. Technical and computational details are summarized in subsection 2.5.

2. METHOD

2.1 Theory

A new tight-binding Hamiltonian-based method using Mathlab code is presented in this work. It shows carrier delocalization at the Graphene Dirac point, which is helpful to study the electron transport and magnetic properties of the 2D materials. Graphene forms a honeycomb lattice consisting of a layer of carbon atoms, which can be described by the following Hamiltonian

$$H_{TB} = \sum_A \varepsilon_A C_A^\dagger C_A + \sum_{\langle A,B\rangle}\left[t_{AB} C_A^\dagger C_B + t_{AB}^* C_A C_B^\dagger\right] \quad (1)$$

where $(C_A^\dagger)C_A$ creates (annihilates) an electron at the site A with on-site energy ε_A, and the sum is taken only between nearest-neighbor sites A and B, with hopping energy t_{AB}.[1] For the practical purpose we use atomic unit system. As the origin of the energy, the value of $\varepsilon_A$is set to be zero and the value of the t is fixed to be t = 2.8 eV ($0.103\ a.u$)..[2,3] Considering an infinite graphene sheet in the absence of external potential and magnetic fields, one obtains the energy band structure of graphene from finding the eigenvalues of the tight-binding (TB) Hamiltonian Eq (1), as

$$E(\vec{k}) = \pm t\sqrt{3 + f(\vec{k})}, \quad (2)$$

where $$E^{+} = t\sqrt{3 + f(\vec{k})}, \quad (3)$$

$$E^{-} = -t\sqrt{3 + f(\vec{k})}, \quad (4)$$

and

$$f(\vec{k}) = 2\cos(\sqrt{3}K_y a) + 4\cos\left(\frac{\sqrt{3}}{2}K_y a\right)\cos\left(\frac{3}{2}K_x a\right) \quad (5)$$

Here, a represents the carbon-carbon distance in graphene which is 1.42 Å. According to Eq (2), the energy band structure is gapless in six points of the reciprocal space where $|E^{+}(k) - E^{-}(k)| = 0$, from which only two points are inequivalent, labeled as K and K'. The dependence of energy spectrum on the wave vector $\vec{k}$ is almost linear in the vicinity of each of these points.[30]

2.2 Static properties

In the basis of eigenstates of the TB Hamiltonian and in the absence of external magnetic field, Hamiltonian takes the form for electrons

$$H_i^{+} = H_i^{0} = E_i^{+}(k_x, k_y) \quad (6)$$

and for holes $$H_j^{-} = H_j^{0} = E_j^{-}(k_x, k_y) \quad (7)$$

Here, '+' and '-' signs present the occupied and unoccupied bands respectively.

Total Hamiltonian is

$$\widehat{H}_{TB} = \sum_i H_i^{+}|i\rangle\langle i| + H_j^{-}|j\rangle\langle j| = \sum_i E_i^{+}|i\rangle\langle i| + E_j^{-}|j\rangle\langle j| \quad (8)$$

Each $|i\rangle\langle i|$ and $|j\rangle\langle j|$ is projector operator in the basis of eigenstate of H_i^{+} and H_j^{-} with energy E_i^{+} and E_j^{-}, respectively, where the indices $i = 1, 2, 3, \ldots$correspond to $LUMO$, $LUMO + 1$, $LUMO + 2, \ldots$ and $j = 1, 2, 3$ correspond to $HOMO, HOMO - 1, HOMO - 2, \ldots$. Here, $LUMO$ and

$HOMO$ stand for lowest unoccupied molecular orbital and highest occupied molecular orbital respectively.

Hereafter, we neglect electron-hole interaction and focus only on one particle, electron. In the presence of magnetic field, Hamiltonian includes the interaction term

$$\hat{H} = \hat{H}_{TB} - \mu_B \vec{L} \,.\, \vec{B} \tag{9}$$

and the corresponding time-independent Schrödinger equation for one electron is

$$\left(H_{TB} - \mu_B \vec{L} \,.\, \vec{B}\right)\varphi_i(k_x, k_y) = \varepsilon_i \varphi_i(k_x, k_y) \tag{10}$$

Here, we use $\vec{B} = (0,\ 0,\ B_z)$,

and $\vec{L} = (0,\ 0,\ L_z)$

In position space, $\hat{L}_z = -i\left(\frac{\partial}{\partial x} y - x \frac{\partial}{\partial y}\right)$

and in momentum space, $\hat{L}_z = -i\left(k_x \frac{\partial}{\partial k_y} - \frac{\partial}{\partial k_x} k_y\right)$

In Eq (10), ε_i is the eigenenergy and $\varphi_i(k_x, k_y)$ is the eigenstate in k-space. At zero magnetic field, eigenstates of Hamiltonian (9) are at the same time eigenstates of the momentum operator. However, at nonzero values of magnetic field, the eigenstates $\varphi_i(k_x, k_y)$ are defined at several values of momentum, while momentum is not a good quantum number anymore. The solution of this equation provides stationary eigenstates, which do not change in time. The tools for analysis of E_i and $\varphi_i(k_x, k_y)$ are shown in observable section.

2.3 Quantum Dynamics

However, in case the system is prepared in the initial state which does not coincide with any of the stationary state $\psi(k_x, k_y, t) \neq \varphi_i(k_x, k_y)$, one uses more general time-dependent

Schrödinger equation (TDSE) for description of time evolution of nonstationary states. Here, the TDSE reads

$$i\hbar \frac{d}{dt} \psi(k_x, k_y, t) = \left(H_{TB} - B\hat{L}_z\right) \psi(k_x, k_y, t) \quad (11)$$

One solves the time-dependent Schrödinger equation by propagating wave function during infinitesimal time step τ

$$\psi(k_x, k_y \ \ t + \tau) = \boldsymbol{U}(\tau)\, \psi(k_x, k_y, t) \quad (12)$$

by the time evolution operator

$$\boldsymbol{U}(\tau) = \exp\left(-\frac{i}{\hbar} H\tau\right) = \exp\left(-\frac{i}{\hbar}\left(H_{TB} - B_z\hat{L}_z\right)\tau\right) \quad (13)$$

On the account of the initial conditions, we explore specific class of the initial wavefunctions in 2D momentum space represented as a product of 1D Gaussian functions, specified by the values of initial momentum k_{x_0}, k_{y_0},and initial positions x_0, y_0, and width parameter σ

$$\psi_0(k_x, k_y, t = 0) = \psi(k_x)\psi\left(k_y\right) \quad (14)$$

$$\psi(k_x) = N\exp[ix_0\left(k - k_{x_0}\right)] \exp[-\frac{\left(k_x - k_{x_0}\right)^2\sigma}{4}] \quad (15a)$$

$$\psi\left(k_y\right) = N\exp[iy_0\left(k_y - k_{y_0}\right)] \exp[-\frac{\left(k_y - k_{y_0}\right)^2\sigma}{4}] \quad (15a)$$

Once we have the eigenstates, we can calculate electron dynamics of probability density as function of the magnetic field by taking the absolute value square of orbitals.

2.4 Observables

The tight-binding Hamiltonian is used in momentum space to calculate time-independent and time-dependent population density analysis. Eigenstates can be studied at various values of the applied magnetic field. When magnetic field applied, eigenstates and eigenvalues change with different values of magnetic field. Eigenvalues of energies can be converted into the density of states (DOS) in order to study the influence of magnetic field in visual form. The partial density of states for the given band is defined as

$$D_{band}(\varepsilon) = \sum_i \delta(\varepsilon - \varepsilon_i) \tag{16}$$

where the energy of a given eigenstate is ε_i and the index i runs over all calculated eigenstates. The Dirac delta function $\delta(\varepsilon - \varepsilon_i)$ is modeled using a Lorentzian:

$$\delta(x) = \frac{1}{\pi}\frac{\sigma}{\sigma^2 + x^2} \tag{17}$$

The total density of states (DOS) was calculated as a sum of partial DOS:

$$D(\varepsilon) = \sum_{band} D_{band}(\varepsilon) \tag{18}$$

The absorption spectra are calculated, and the most probable excitations are identified using the following equation:

$$\alpha(\omega) = \sum f_{HO,i;LU,j}\ \delta(|\varepsilon_{HO,i} - \varepsilon_{LU,j}| - \hbar\omega) \tag{19}$$

where, $f_{HO,i;LU,j} = c\left|\vec{D}_{HO,i;LU,j}\right|^2$;

$$D^x_{HO,i;LU,j} = \int dk_x \int dk_y \varphi_i^*(k_x, k_y).k_x.\varphi_j(k_x, k_y)$$

and $D^y_{HO,i;LU,j} = \int dk_x \int dk_y \varphi_i^*(k_x, k_y).k_y.\varphi_j(k_x, k_y)$

Then, trajectories of expectation values of momentum $\langle P_x\rangle(t)$ and $\langle P_y\rangle(t)$ in the presence of magnetic field can be calculated by using the following initial conditions –

$$\langle P_x\rangle(t) = \left\langle \psi(k_x, k_y, t)\middle|\hat{P}_x\middle|\psi(k_x, k_y, t)\right\rangle \tag{20a}$$

$$\langle P_y \rangle(t) = \left\langle \psi(k_x, k_y, t) \middle| \hat{P}_y \middle| \psi(k_x, k_y, t) \right\rangle \qquad (20b)$$

Here, $\hat{P}_x = -i\frac{\partial}{\partial x}$ and $\hat{P}_y = -i\frac{\partial}{\partial y}$ stand for projections of momentum operators onto x and y cartesian directions. The ranges of $\mathrm{k_x}$ and $\mathrm{k_y}$ are $-\frac{|\mathrm{b_2}|}{2} < \mathrm{k_x} < \frac{|b_2|}{2}$ and $-\frac{(1-\sqrt{3})|\mathrm{b_2}|}{2} < \mathrm{k_y} < \frac{(1-\sqrt{3})|b_2|}{2}$ respectively. Since $|b_2| = |b_2| = |b| = \frac{4\pi}{3a}$, these can be written as $-\frac{|b|}{2} < \mathrm{k_x} < \frac{|b|}{2}$ and $-\frac{(1-\sqrt{3})|b|}{2} < \mathrm{k_y} < \frac{(1-\sqrt{3})|b|}{2}$.

2.5 Computational Details

Electron dynamics in 2D momentum space in the presence of normally incident magnetic field is calculated by the code implementing equations 1-20 using MATLAB software. We consider 2D rectangular lattice with 3025 grid points while number of grid points along both k_x and k_y is 55. The full-scan bands for 2D momentum which are $-\frac{|b|}{2} < \mathrm{k_x} < \frac{|b|}{2}$ and $-\frac{(1-\sqrt{3})|b|}{2} < \mathrm{k_y} < \frac{(1-\sqrt{3})|b|}{2}$; fine grid points are considered with the step size $\frac{|b|}{55}$ and $\frac{(1-\sqrt{3})|b|}{55}$ along k_x and $k_y$respectively. For the dynamics calculations, the total number of time steps is 2040 and the duration of each time steps selected is $0.5\ a.u.$ So, the duration of whole trajectory is $24.67\ fs$. Here, we keep time steps short to keep reliable precision. To fully identify the complete cyclotron density distribution, the longer intervals of dynamics need to be considered.

We compute energy band structure of graphene, using tight-binding Hamiltonian according to equation (1) [in method section]. In this section, we will get input parameters of tight-binding Hamiltonian. Graphene consists of carbon atoms arranged in honeycomb lattice. It has triangular lattice structure with a basis of two atoms per unit cell as shown in **Figure S1 (a)**. The lattice vectors can be represented as

$$\vec{a}_1 = \frac{a}{2}(3,\sqrt{3}), \quad \vec{a}_2 = \frac{a}{2}(3,-\sqrt{3}) \text{ (21a)}$$

The reciprocal lattice-vectors can be present as

$$\vec{b}_1 = \frac{2\pi}{3a}(1,\sqrt{3}), \qquad \vec{b}_2 = \frac{2\pi}{3a}(1,-\sqrt{3}) \quad \text{(21b)}$$

Each carbon atom has three nearest-neighbor and six next-nearest neighbor atoms. **Figure S1 (b)** shows the Brillouin zone (BZ) of graphene which consists two points K and K' at the corners called Dirac points.[8] By solving equation (1) [in method section], one can obtain energy band structure of graphene as function of momentum.

The energy band structure of graphene, according to Eq (2-4) is shown in **Figure S1 (c)**. At Dirac points, valence band (VB) and conduction band (CB) touch each other. The electron dispersion relation is linear around these points.[9] The conical in **Figure S1 (d)** shows the zoomed in schematic of energy bands around one of the Dirac points. It shows that VB and CB overlap at points K and K'. In graphene, three valence electrons form σ-bonds with three neighboring carbon atoms and the fourth electron forms π-bond normal to the plane of the σ-bonds. Since the π-bond electrons are relatively weakly bound to the nuclei and are delocalized over the graphene structure, they contribute to electronic properties of graphene.[i]

3 Discussion

In this study, we perform computational modeling of the photo-excited electron dynamics in graphene using the evolution operator for wave function in momentum space under interaction with applied magnetic fields. We develop and test a methodology for calculating electron probability density in graphene with applied magnetic fields. The application of magnetic fields across graphene can induce the splitting of degenerate Landau levels resulting in energetic control spin states. This application is highly important to the development of materials for quantum computing applications and electronic security. Moreover, we demonstrate that the presented

method can identify perturbation of the electronic structure of graphene by applying varying strengths of magnetic fields. With the increasing magnetic field strengths, it is expected that the the energies of electronic states will be modified so that field induced effect will dominate and Landau levels will be created. The perturbation of electronic states is decreasing with the decreasing values of the magnetic field. One may set an approximate criterion as follows: interaction with magnetic field should be much smaller than energy difference of the CB in gamma point and Dirac point. The used values of the magnetic field are too high for practical miniature devices. We consider these high values to save computational resources and explore the shorter duration of trajectories. It is expected that simulation of longer time intervals will enable additional details and reveal closed-loop trajectories. The methodology used in this work can be extrapolated for spin-dependent treatment. This direction of further development is one in the list of several possible improvements such as including phonon-induced relaxation. Including spin would allow computing magnetization as a sum of contributions from partial motion and spin polarization. Coulomb Scattering in the Dirac point vicinity occurs upon ultrafast photoexcitation for the values of excitation energy at which energy of a single carrier is sufficient for creating additional electron-hole pair. The Multielectron generation process is not considered in this work while we consider one-particle interaction with the magnetic field. Multielectron effects can be added in future work using our published methodology.[4] The magnetism of material can originate from multiple causes such as nuclear magnetism, electrons with unpaired spins on certain ions, the angular momentum of atomic orbitals, and long-range currents. In this work, we focus only on the last aspect and assume other aspects are included into the pre-computed momentum dispersion. Our future work will include explicit treatment of electrons with unpaired spins. There is a deviation from ideal solution due to rectangular grid points. Circles (continuous closed loops) are represented with a

pattern of discrete grid points. For a square grid and a small number of points, a circular pattern looks like a rectangle.

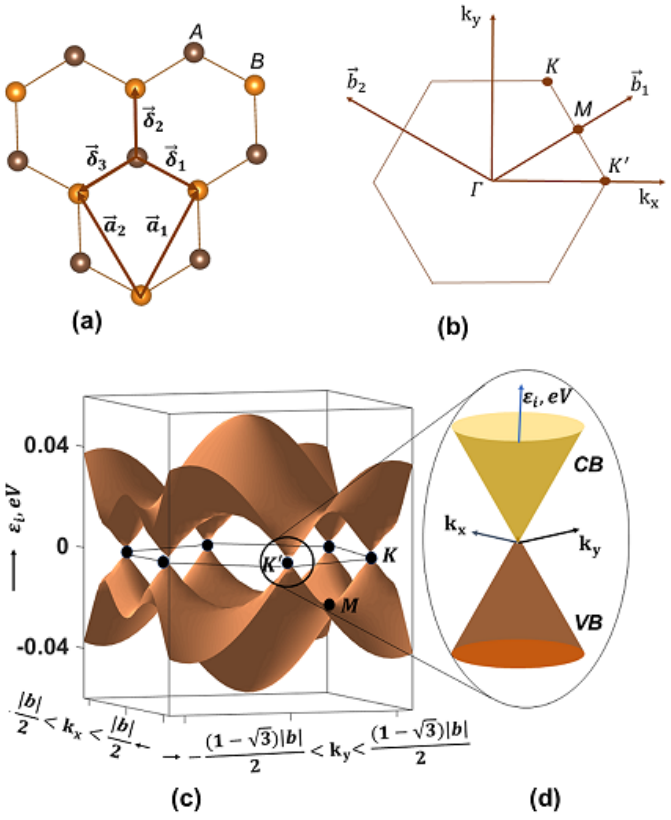

Figure S1: (a) Honeycomb lattice structure of 2D graphene. The graphene lattice structure consists of two interpenetrating triangular lattices A and B. The direct lattice vectors of graphene are $\vec{a}_1$ and $\vec{a}_2$, and nearest neighbor vectors are $\delta_i, i = 1, 2, 3$. (b) Schematic of the first BZ of the reciprocal lattice of graphene with Dirac cones at points K' and K . The ranges of in which k_x and k_y change are $-\frac{|b|}{2} < k_x < \frac{|b|}{2}$ and $-\frac{(1-\sqrt{3})|b|}{2} < k_y < \frac{(1-\sqrt{3})|b|}{2}$ respectively. (c) Energy dispersion spectrum of graphene. The CB (lower band) and the CB (upper band) touch each other at the corners (Dirac points) of BZ. (d) Energy band is zoomed-in close to one of the Dirac points. The range of energies in y-axis is $-0.06(-0.0022) - 0.06(-0.0022\ a.u)\ eV$.

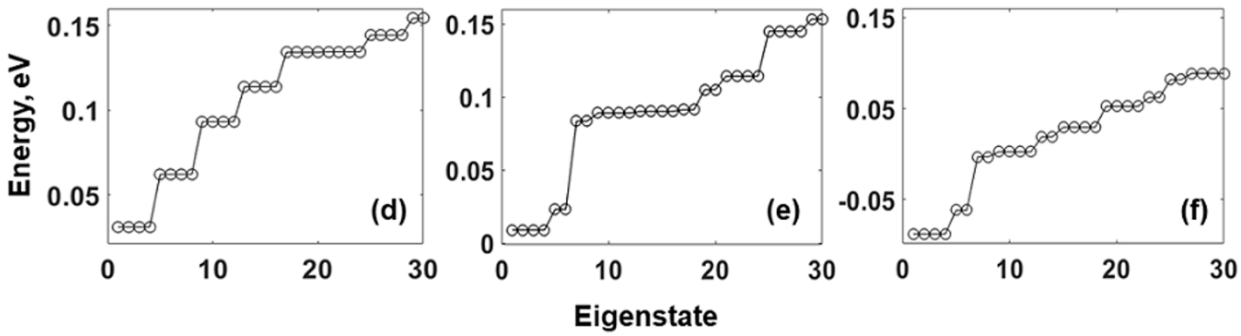

Figure S2: The energies of the initial thirty eigenstates at the same values of the magnetic field B=0, .7, 1.93 T. Note that as the value of the magnetic field increases, the energy of the lowest eigenstate decreases. The computed dependence on the magnetic field prompts sensitivity of the conductivity/resistivity of graphene to the magnetic field.

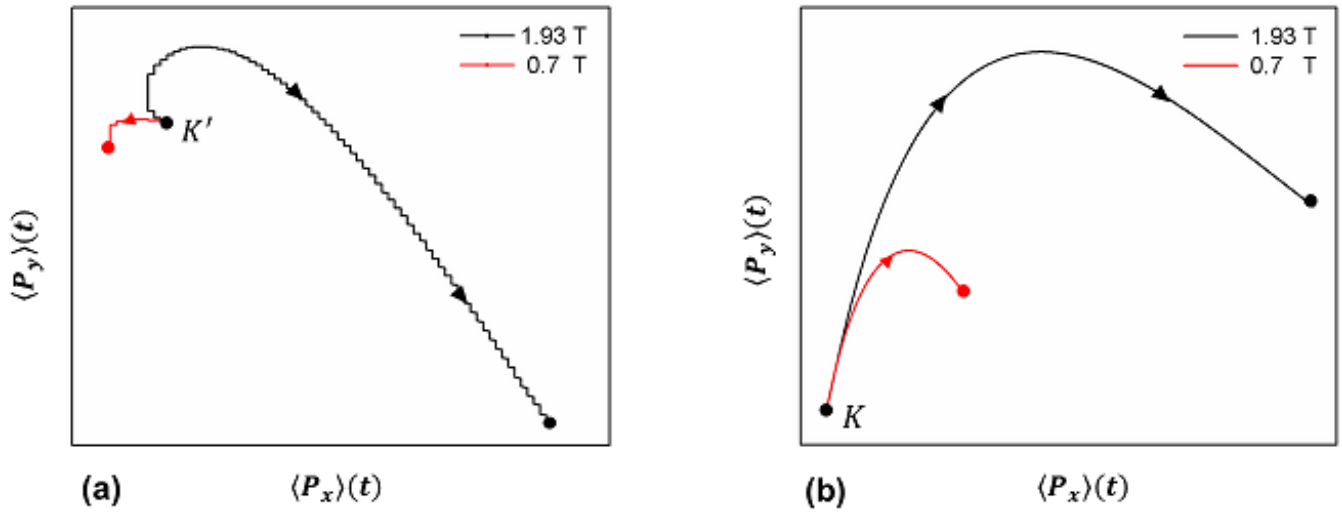

Figure S3: (a) Expectation values of momentum trajectories start at K' point in the presence of magnetic field $B = 0.7\ T$ and $1.93T$. The trajectories of expectation values of momentum start at K'point and travel opposite directions. (b) Expectation values of momentum trajectories start at K point in the presence of magnetic field $B = 0.7\ T$ and $1.93\ T$. The trajectories of the expectation value of momentum start at K point and travel along the same direction. Arrowheads indicate the direction of trajectories.

Table of Contents

I. Animated movie of eigenstates and their corresponding energies at first Brillouin zone of reciprocal space in the presence of magnetic field $B = 0.7\,T$. Here, blue and yellow colors represent zero and maximum electron probability density respectively.

II. Animated movie of eigenstates and their corresponding energies at first Brillouin zone of reciprocal space in the presence of magnetic field $B = 1.93\,T$. Here, blue and yellow colors represent zero and maximum electron probability density respectively.

III. Animated movie of electron dynamics of probability density with time propagation in 2D momentum space in the presence of magnetic field $B = 0.7\,T$. Here, blue and yellow colors represent zero and maximum electron probability density respectively.

IV. Animated movie of electron dynamics of probability density with time propagation in 2D momentum space in the presence of magnetic field $B = 1.93\,T$. Here, blue and yellow colors represent zero and maximum electron probability density respectively.

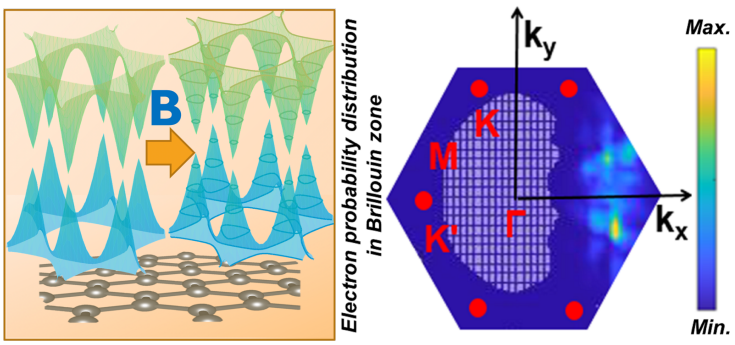

References

(1) Chaves, A.; Covaci, L.; Rakhimov, K. Y.; Farias, G. A.; Peeters, F. M. Wave-Packet Dynamics and Valley Filter in Strained Graphene. *Phys. Rev. B.* **2010**, *82*, 205430.

(2) Castro Neto, A. H.; Guinea, F.; Peres, N. M. R.; Novoselov, K. S.; Geim, A. K. The Electronic Properties of Graphene. *Rev. Mod. Phys.* **2009**, *81*, 109–162.

(3) Hosseingholipourasl, A.; Hafizah Syed Ariffin, S.; Al-Otaibi, Y. D.; Akbari, E.; Hamid, F.; Koloor, S.; Petrů, M. Analytical Approach to Study Sensing Properties of Graphene Based Gas Sensor. *Sensors.* **2020**, *20*, 1506.

(4) Castro Neto, A.; Guinea, F.; Peres, N.; Novoselov, K.; Geim, A. Rev. Mod. Phys. 81, 109 (2009): The Electronic Properties of Graphene. *Rev. Mod. Phys.* **2009**.